Large Increase in External Quantum Efficiency by Dihedral Angle Tuning in a Sky#Blue Thermally Activated Delayed Fluorescence Emitter

DOI: 10.1002/((please add manuscript number))
Article type: Communication

Large Increase in External Quantum Efficiency by Dihedral Angle Tuning in a Sky-Blue Thermally Activated Delayed Fluorescence Emitter

Wenliang Huang[†,‖,#,*], *Markus Einzinger*[‡,#,*], *Andrea Maurano*[§], *Tianyu Zhu*[†], *Jan Tiepelt*[‡], *Chao Yu*[‖], *Hyun Sik Chae*[§], *Troy Van Voorhis*[†,*], *Marc A. Baldo*[‡,*] *and Stephen L. Buchwald*[†]

† Department of Chemistry, ‡ Department of Electrical Engineering and Computer Science, Massachusetts Institute of Technology, Cambridge, Massachusetts 02139, United States
E-mail: meinzing@mit.edu, tvan@mit.edu, baldo@mit.edu

‖ Beijing National Laboratory for Molecular Sciences, College of Chemistry and Molecular Engineering, Peking University, Beijing 100871, P. R. China
E-Mail: wlhuang@pku.edu.cn

§ Advanced Materials Lab (AML), Samsung Advanced Institute of Technology (SAIT) America, Burlington, MA 01803, United States

# Equal contribution
* Corresponding author

Keywords: Organic Light Emitting Diode, Thermally Activated Delayed Fluorescence, Dihedral Angle Tuning, Molecular Design, Blue Emitter

Efficient and stable blue emitters for organic light-emitting diodes are urgently needed for next-generation display and lighting applications. The discovery of thermally activated delayed fluorescence (TADF) has revealed a new class of promising candidates. After pairing the iminodibenzyl donor with the triazine acceptor *via* a phenylene linker, we employ dihedral angle tuning to regulate the difference between the energy levels of singlet and triplet excited states. We observe enhanced reverse intersystem crossing rates in response to increased methylation at the phenylene linker. This behavior agrees with our density functional theory calculations. Photoluminescence quantum yields of up to 98% are achieved upon doping into a solid-

state matrix. When incorporated in devices, the maximum external quantum efficiency is 28.3% for the emitter with the most favorable trade-off between singlet-triplet splitting and fluorescent oscillator strength. This result highlights the general applicability of dihedral angle tuning, a molecular design strategy that could be used to improve the performance of donor-acceptor type TADF emitters without significantly changing their emission spectra.

Organic light-emitting diodes (OLEDs) are an established light source in the display industry.[1] In state-of-the-art products, red and green colors are generated using phosphorescent emitters, which enable internal quantum efficiencies (IQEs) of up to 100%.[2,3] However, they rely on the use of expensive noble metals.[4] Moreover, blue phosphorescent emitters degrade rapidly, which results in low operational lifetimes.[5] As a consequence, blue colors are currently being produced by fluorescent emitters. Those emitters have long been limited to internal quantum efficiencies of 25%, but can reach internal quantum efficiencies of up to 62.5% by employing triplet fusion.[6,7]

Thermally activated delayed fluorescence is a more efficient alternative to classical fluorescence and it can exhibit IQEs up to 100%.[8–11] In devices, three quarters of excitons are statistically formed in a triplet state, which are non-emissive in case of fluorescent emitters.[12] TADF molecules harness both singlet and triplet excitons by introducing appreciable reverse intersystem crossing (RISC) to convert non-emissive triplet excitons to emissive singlet excitons.[13,14] By spatially separating the highest occupied molecular orbital (HOMO) and lowest unoccupied molecular orbital (LUMO), the exchange energy is lowered and singlet-triplet splitting ($\Delta E_{ST} = E_{S1}-E_{T1}$) is reduced.[8] As a consequence, the singlet state becomes thermally accessible from the triplet state at room temperature. It has also been revealed that the resulting RISC proceeds via vibronic coupling of the triplet charge transfer

state (^{3}CT) state with a triplet localized exciton state (^{3}LE), which in turn couples to the singlet manifold.[15] While many TADF molecules have been reported,[16–22] widely applicable molecular design principles beyond trial-and-error approaches remain scarce.[23–25] Recently, Adachi, *et al.*[26] and we[27] have shown that it is possible to enhance RISC in blue fluorescent molecules with carbazole donors by dihedral angle tuning (Figure 1a, b). The dihedral angle between donor and linker (θ_1) and the dihedral angle between linker and acceptor (θ_2) can be tuned by attaching methyl groups to the phenylene linker. Advantageously, this can be done without significantly changing emission wavelengths. As a result, deep blue emitters with external quantum efficiencies slightly above 10% were obtained. Herein, we report our latest efforts to test the general validity of the dihedral angle tuning strategy by applying it to a promising novel donor-linker-acceptor-type molecule. We employed iminodibenzyl (**IDB**) as a donor and paired it with the common acceptor triazine (**TRZ**) with a phenylene linker. This facilitated gradual adjustment of the dihedral angle between donor and acceptor by changing the number of methyl groups on the phenylene linker.

A practical protocol for *N*-arylation of iminodibenzyl using palladium catalysts was recently reported.[28] This method provides an entry point to synthesize targeted IDB-TRZ compounds, including those with high steric hindrance (Figure 1c). Four compounds, **IDB-TRZ-H** (**1**), **IDB-TRZ-Me** (**2**), **IDB-TRZ-Me$_2$** (**3**), **IDB-TRZ-Me$_4$** (**4**) were selected. Thermogravimetric analysis (TGA) confirms the high thermal stability for all four compounds (see Figure S1 for details). Compounds **1-4** represent different degrees of methyl substitution at the phenylene linker, which is anticipated to influence the dihedral angles between the donor, the linker, and the acceptor. This is confirmed by density functional theory (DFT). The ground state geometry was optimized in the gas phase, followed by a

single point calculation (for details, see experimental section). The calculated structures of compounds **1**-**3** show a gradual increase of the dihedral angles between iminodibenzyl donor and phenylene linker (θ_1) from 71.8º for **1**, to 76.4º for **2**, and eventually 78.4º for **3**, while phenylene linker and triazine acceptor are nearly coplanar for these three compounds with θ_2 close to zero (Table 1). The addition of two methyl groups *ortho* to triazine in compound **4** results in the phenylene linker being almost orthogonal to both the iminodibenzyl donor (θ_1=78.0°) and triazine acceptor (θ_2=79.2°).

The electron-donating strength of iminodibenzyl was estimated from DFT calculations, which yielded a HOMO energy of -4.95 eV, indicating it is a stronger donor than carbazole (-5.44 eV) and diphenylamine (-5.08 eV) but a weaker donor compared to 9,9-dimethyl-9,10-dihydroacridine (-4.88 eV).[23] The lowest triplet energy level of the isolated iminodibenzyl donor was calculated to be 3.18 eV. Then, to predict the ΔE_{ST} and oscillator strength (*f*) of compounds **1**-**4**, we also performed time-dependent density function theory (TDDFT). The results are listed in Table 1. With the least steric hindrance, compound **1** has a large oscillator strength of 0.155 but its ΔE_{ST} value of 138 meV is not small enough for strong TADF. For compound **2**, the addition of a methyl on the phenylene linker *ortho* to iminodibenzyl led to a more twisted structure due to the increased steric hindrance. As a result, the ΔE_{ST} is decreased to 112 meV, which suggests enhanced TADF character for compound **2**. In compound **3**, the ΔE_{ST} is further reduced to 94 meV by adding one more methyl at the other *ortho* position to iminodibenzyl. Meanwhile, the *f* values of compounds **2** and **3** remain high at 0.118 and 0.093, respectively, because of the flexible structure of the iminodibenzyl donor. The molecular orbitals of the compounds **1**-**4** from DFT calculations are shown in Figure 2, which reveals that the HOMO and LUMO are increasingly separated due to the dihedral angle tuning. Please refer to Figures S2-6 for the isosurface plots of the molecular orbitals and

natural transition orbital (NTO) analysis. Tables S1-2 show a full Mulliken population analysis, revealing the percentage contribution of each component to HOMO and LUMO. Compound **4** has a near zero ΔE_{ST} of 2 meV but a low oscillator strength as the triazine acceptor and the phenylene linker are almost orthogonal. Therefore, we expect it to be not as effective as a TADF emitter compared to compound **3**, which has a favorable combination of relatively small ΔE_{ST} and large *f* value.

The steady-state absorption spectra for the toluene solutions of compounds **1**-**4** are shown in Figure 3a. Compounds **1**-**3** show a broad absorption peaking between 350 and 400 nm, corresponding to an intramolecular charge transfer (ICT) transition. In accordance with our DFT calculations, the intensity of the ICT absorption decreases with increasing dihedral angle. Notably, the absence of this ICT transition in compound **4** is attributed to the vanishing oscillator strength as predicted by DFT. Photoluminescence (PL) spectra showed blue to sky-blue emission for all four compounds peaking between 450 and 480 nm (Figure 3b). Compound **1** shows a hypsochromic shoulder, which we attribute to different conformers in solution, since this shoulder becomes less pronounced when the compound is doped into a solid state matrix (Figure S7). The decreasing Stokes shifts in compounds **1**-**4** indicates that structural rigidity is enhanced by the addition of methyl groups at the phenylene linker.

Time resolved transient PL spectra and photoluminescence quantum yield (PLQY) data were collected using doped films of 20% emitter (compounds **1**-**4**) in bis(diphenylphosphoryl)dibenzo[b,d]furan (PPF) (Figure 3cd). The time resolved transient PL spectra showed two distinct trends. Firstly, the delayed lifetime monotonically decreases with increasing number of methyl groups (Table 2); Secondly, the intensity of the delayed emission is enhanced accordingly. The RISC rates were calculated using the transient PL and PLQY data of compounds **1**-**4** according to Equation S4**.** The RISC rates of compounds **1**-**4**

are enhanced throughout the series. Since RISC rates are known to increase exponentially with decreasing ΔE_{ST}, this supports our design strategy by applying dihedral angle tuning to reduce ΔE_{ST}. Moreover, the increased structural rigidity leads to an increase of PLQYs for compounds **1**-**3** from 17% for **1**, to 68% for **2**, and ultimately 98% for **3**. The PLQY of compound **4** is considerably lower at 37%. This is consistent with a very small *f* value for compound **4** as calculated by TDDFT, which indicates a slow $S_1 \rightarrow S_0$ transition, competing less successfully with nonradiative decay pathways. Overall, the appreciable RISC rate of $6.4 \cdot 10^4$ and high PLQY of 98% for compound **3** suggests that it should be the best TADF emitter among compounds **1**-**4**. We confirmed that both prompt and delayed emission originates from S_1, as evidenced by the spectra shown in Figure S8. To experimentally confirm ΔE_{ST}, we recorded fluorescence and phosphorescence spectra of compounds **1**-**4** doped in drop-casted films of poly(methylmethacrylate) (PMMA) at low temperature (15K), shown in Figure S9. The extracted ΔE_{ST} values show very good agreement with TDDFT (Table 1).

In order to verify that these trends also translate into devices, we fabricated OLEDs with identical device structures. We employed the layer stack indium tin oxide (ITO) (100 nm) / N,N′-Di(1-naphthyl)-N,N′-diphenyl-(1,1′-biphenyl)-4,4′-diamine (NPB) (50 nm) / 1,3-Bis(N-carbazolyl)benzene (mCP) (10 nm) / 20% Emitter (compounds **1**-**4**) in 2,8-Bis(diphenylphosphoryl)dibenzo[b,d]furan (PPF) (30 nm) / 1,3,5-Tri(m-pyridin-3-ylphenyl)benzene (TmPyPb) (30 nm) / Lithium Fluoride (LiF) (1 nm) / Aluminum (Al) (100 nm) (Figure S10). External quantum efficiencies (EQEs) as a function of current density for these devices are plotted in Figure 4a. Compounds **1**-**3** exhibit maximum EQEs of 6.8%, 12.3%, and 28.3%, respectively. This constitutes a fourfold improvement upon dihedral angle tuning by adding methyl groups on the phenylene linker. Besides dihedral angle tuning, we

also attribute the enhancement of EQE to increased structural rigidity as a result of methylation at the phenylene linker, which should reduce the loss pathways of nonradiative decay. It is noteworthy that compound **3** still shows a very high EQE of 14.7% at 1000 cd/m^2. Compound **4** still shows a respectable maximum EQE of 16.4% despite its low PLQY, which is likely due to highly efficient RISC with a rate of $1.2 \cdot 10^6$, almost 20 times larger than that of compound **3**. In addition, other underlying mechanisms, such as the optical microcavity effect[29] or the horizontal orientation of transition dipole moments[30] of compound **4** in the OLED devices may also play a role. The electroluminescent (EL) spectra of compounds **1**-**4** are similar to their PL spectra with peaks between 484 and 496 nm (see Figure 4b). The electrical properties of the device were not significantly altered by different emitters (see Figure 4cd). EQE, current efficiency and power efficiency at different luminance levels can be found in Table S3. For all four compounds, the shapes of the electroluminescence spectra do not appreciably change when the current density is varied (Figures S11-14).

In summary, we have demonstrated that iminodibenzyl can be employed as a strong donor together with a triazine acceptor to realize highly efficient TADF emitters. We applied the molecular design strategy of dihedral angle tuning, which reduced ΔE_{ST} and led to a faster rate of RISC. This strategy is aided by theoretical predictions and verified by time-resolved spectroscopy and PLQY measurements. Employing the IDB-TRZ molecules in OLEDs yields a fourfold increase in EQEs upon methyl addition at the phenylene linker with a maximum EQE of 28% for compound **3**, the highest value achieved by the dihedral angle tuning strategy and among the highest values reported to date for sky-blue emitters in OLEDs. We anticipate that this molecular design strategy based on dihedral angle tuning should be readily applicable to other systems to improve device efficiencies.

Experimental section

DFT: All DFT computations were carried out using the Q-Chem 4.4 software package.[31] The gas-phase ground state geometry optimizations were performed using the B3LYP exchange-correlation functional[32] in the 6-31G* basis set.[33] Then TDDFT was adopted at the same level to estimate the excitation energies in toluene by using the polarizable continuum model (PCM).[34] We used a dielectric constant of 2.38 and 302 PCM grid points. We used a large integration grid (99,590) for the geometry optimizations. Please see SI for more details.

Synthesis: The synthetic protocols for compounds **1-4** followed the general methods developed by Buchwald, et al.[28] The syntheses of **TRZ-Br** and its methyl derivatives were done according to literature procedure.[27] The *N*-arylation of iminodibenzyl was conducted using 1.1 equivalents of lithium bis(trimethylsilyl)amide (LiHMDS) and 1 mol% **Pd-RuPhos-G4** for compounds **1-3** or 2 mol% **Pd-RuPhos-G4** for compound **4**. The synthesis of compound **1** is shown here as an example. Please see SI for details about synthesis, characterization and NMR spectra of compounds **1-4**. Preparation of compound **1**: In a nitrogen-filled glovebox, lithium bis(trimethylsilyl)amide (LiHMDS, 129 mg, 0.147 mmol, 1.1 equiv.) was added to a reaction tube (Fisherbrand™ Disposable Borosilicate Glass Tubes with Threaded End, from Fisher Scientific, Catalog No. 14-959-37C) equipped with a stir bar and then capped with a screw cap (Kimble™ Black Phenolic Unlined Screw Thread Closures with Open Tops, from Fisher Scientific, Catalog No. 03-340-7G) with a septa (from Fisher Scientific, Catalog No. 03-394B). The reaction tube was removed from the glovebox. Iminodibenzyl (137 mg, 0.70 mmol, 1.0 equiv.), **Pd-RuPhos-G4** (6.0 mg, 0.007 mmol, 1.0 mol%), and **TRZ-Br** (272 mg, 0.70 mmol, 1.0 equiv.) were weighed out on bench-top and added to the reaction tube. The reaction tube was recapped with the septum and then was

alternately evacuated and refilled with argon (this process was repeated a total of three times). To the reaction mixture was added 1,4-dioxane (2.0 mL) via syringe under an argon atmosphere. The mixture was stirred while the reaction vessel was heated in an oil bath at 100 ºC for 16 h. After allowing to cool to room temperature, the mixture was subjected to a kinetic quench by dilution with CH_2Cl_2 (5.0 mL) and filtered through a short plug of silica gel to remove the insoluble solids. The filtrate was concentrated *in vacuo* with the aid of a rotary evaporator to provide the crude product. This material was purified via flash chromatography on silica gel (using a gradient elution 100% hexanes to 25% CH_2Cl_2 in hexanes), followed by trituration using hexanes to yield compound **1** as an off-white solid (305 mg, Yield: 87%).

Device Fabrication: Detailed description of device fabrication can be found in our previous publication.[35]

Measurements: Absorption spectra were measured from solution in toluene (2M) in a UV–vis–NIR spectrophotometer (Cary 5000, Agilent). Emission spectra were measured from the same solution using a spectrometer (SP2300, Princeton Instruments) with a 340-nm-emitting LED as excitation source (LED, M340L4, Thorlabs). For a detailed description of PLQY measurements, time-resolved PL measurements and device measurements, please refer to our previous publication.[35]

Supporting Information

Supporting Information is available from the Wiley Online Library or from the authors.

Acknowledgements

Research reported in this publication was funded by Samsung Electronics. M.E., T. Z. and J.T. were supported by the U.S. Department of Energy, office of Basic Energy Sciences (Award No. DE-FG02-07ER46474). We thank Sigma-Aldrich for the generous donation of RuPhos. The authors would like to thank Yuntong Zhu for help with the TGA measurements.

Conflict of Interest

The authors declare no conflict of interest.

Received: ((will be filled in by the editorial staff))
Revised: ((will be filled in by the editorial staff))
Published online: ((will be filled in by the editorial staff))

References

[1] T. Tsujimura, *OLED Display Fundamentals and Applications*, John Wiley & Sons, Inc., Hoboken, USA, **2017**.
[2] M. A. Baldo, D. F. O'Brien, Y. You, A. Shoustikov, S. Sibley, M. E. Thompson, S. R. Forrest, *Nature* **1998**, *395*, 151.
[3] C. Adachi, M. A. Baldo, M. E. Thompson, S. R. Forrest, *J. Appl. Phys.* **2001**, *90*, 5048.
[4] H. Yersin, *Highly Efficient OLEDs with Phosphorescent Materials*, John Wiley & Sons, Weinheim, Germany, **2008**.
[5] D. Jacquemin, D. Escudero, *Chem. Sci.* **2017**, *8*, 7844.
[6] S.-W. Wen, M.-T. Lee, C. H. Chen, *J. Disp. Technol.* **2005**, *1*, 90.
[7] H. Kuma, C. Hosokawa, *Sci. Technol. Adv. Mater.* **2014**, *15*, 034201.
[8] H. Uoyama, K. Goushi, K. Shizu, H. Nomura, C. Adachi, *Nature* **2012**, *492*, 234.
[9] Q. Zhang, B. Li, S. Huang, H. Nomura, H. Tanaka, C. Adachi, *Nat. Photon.* **2014**, *8*, 326.
[10] S. Hirata, Y. Sakai, K. Masui, H. Tanaka, S. Y. Lee, H. Nomura, N. Nakamura, M. Yasumatsu, H. Nakanotani, Q. Zhang, K. Shizu, H. Miyazaki, C. Adachi, *Nat. Mater.* **2015**, *14*, 330.
[11] H. Kaji, H. Suzuki, T. Fukushima, K. Shizu, K. Suzuki, S. Kubo, T. Komino, H. Oiwa, F. Suzuki, A. Wakamiya, Y. Murata, C. Adachi, *Nat. Commun.* **2015**, *6*, 8476.
[12] M. A. Baldo, D. F. O'Brien, M. E. Thompson, S. R. Forrest, *Phys. Rev. B* **1999**, *60*, 14422.
[13] K. Goushi, K. Yoshida, K. Sato, C. Adachi, *Nat. Photon.* **2012**, *6*, 253.
[14] J. Gibson, A. P. Monkman, T. J. Penfold, *ChemPhysChem* **2016**, *17*, 2956.
[15] M. K. Etherington, J. Gibson, H. F. Higginbotham, T. J. Penfold, A. P. Monkman, *Nat. Commun.* **2016**, *7*, 13680.
[16] M. Godumala, S. Choi, M. J. Cho, D. H. Choi, *J. Mater. Chem. C* **2016**, *4*, 11355.
[17] T.-A. Lin, T. Chatterjee, W.-L. Tsai, W.-K. Lee, M.-J. Wu, M. Jiao, K.-C. Pan, C.-L. Yi, C.-L. Chung, K.-T. Wong, C.-C. Wu, *Advanced Materials* **2016**, *28*, 6976.
[18] R. Komatsu, H. Sasabe, Y. Seino, K. Nakao, J. Kido, *J. Mater. Chem. C* **2016**, *4*, 2274.
[19] M. Liu, R. Komatsu, X. Cai, K. Hotta, S. Sato, K. Liu, D. Chen, Y. Kato, H. Sasabe, S. Ohisa, Y. Suzuri, D. Yokoyama, S.-J. Su, J. Kido, *Chem. Mater.* **2017**, *29*, 8630.
[20] Z. Yang, Z. Mao, Z. Xie, Y. Zhang, S. Liu, J. Zhao, J. Xu, Z. Chi, M. P. Aldred, *Chem. Soc. Rev.* **2017**, *46*, 915.
[21] M. Y. Wong, E. Zysman- Colman, *Adv. Mater.* **2017**, *29*, 1605444.
[22] Y. Liu, C. Li, Z. Ren, S. Yan, M. R. Bryce, *Nat. Rev. Mater.* **2018**, *3*, 18020.
[23] Y. Im, M. Kim, Y. J. Cho, J.-A. Seo, K. S. Yook, J. Y. Lee, *Chem. Mater.* **2017**, *29*, 1946.
[24] X.-K. Chen, Y. Tsuchiya, Y. Ishikawa, C. Zhong, C. Adachi, J.-L. Brédas, *Adv. Mater.* **2017**, *29*, 1702767.
[25] C.-Y. Chan, L.-S. Cui, J. U. Kim, H. Nakanotani, C. Adachi, *Adv. Funct. Mater.* **2018**, *28*, 1706023.

[26] L.-S. Cui, H. Nomura, Y. Geng, J. U. Kim, H. Nakanotani, C. Adachi, *Angew. Chem. Int. Ed.* **2017**, *56*, 1571.
[27] W. Huang, M. Einzinger, T. Zhu, H. S. Chae, S. Jeon, S.-G. Ihn, M. Sim, S. Kim, M. Su, G. Teverovskiy, T. Wu, T. Van Voorhis, T. M. Swager, M. A. Baldo, S. L. Buchwald, *Chem. Mater.* **2018**, *30*, 1462.
[28] W. Huang, S. L. Buchwald, *Chem. Eur. J.* **2016**, *22*, 14186.
[29] M. C. Suh, B. Pyo, H. Su. Kim, *Org. Electron.* **2016**, 28, 31-38.
[30] J. Frischeisen, D. Yokoyama, A. Endo, C. Adachi, W. Brütting, *Org. Electron.*, **2011**, 12, 809-817
[31] Y. Shao, L. Fusti Molnar, Y. Jung, J. Kussmann, C. Ochsenfeld, S. T. Brown, A. T.B. Gilbert, L. V. Slipchenko, S. V. Levchenko, D. P. O'Neill, R. A. D. Jr, R. C. Lochan, T. Wang, G. J.O. Beran, N. A. Besley, J. M. Herbert, C. Y. Lin, T. V. Voorhis, S. H. Chien, A. Sodt, R. P. Steele, V. A. Rassolov, P. E. Maslen, P. P. Korambath, R. D. Adamson, B. Austin, J. Baker, E. F. C. Byrd, H. Dachsel, R. J. Doerksen, A. Dreuw, B. D. Dunietz, A. D. Dutoi, T. R. Furlani, S. R. Gwaltney, A. Heyden, S. Hirata, C.-P. Hsu, G. Kedziora, R. Z. Khalliulin, P. Klunzinger, A. M. Lee, M. S. Lee, W. Liang, I. Lotan, N. Nair, B. Peters, E. I. Proynov, P. A. Pieniazek, Y. M. Rhee, J. Ritchie, E. Rosta, C. D. Sherrill, A. C. Simmonett, J. E. Subotnik, H. L. W. Iii, W. Zhang, A. T. Bell, A. K. Chakraborty, D. M. Chipman, F. J. Keil, A. Warshel, W. J. Hehre, H. F. S. Iii, J. Kong, A. I. Krylov, P. M. W. Gill, M. Head-Gordon, *Phys. Chem. Chem. Phys.* **2006**, *8*, 3172.
[32] A. D. Becke, *J. Chem. Phys.* **1993**, *98*, 1372.
[33] P. C. Hariharan, J. A. Pople, *Theoret. Chim. Acta* **1973**, *28*, 213.
[34] M. Cossi, N. Rega, G. Scalmani, V. Barone, *J. Comput. Chem.* **2003**, *24*, 669.
[35] M. Einzinger, T. Zhu, P. de Silva, C. Belger, T. M. Swager, T. Van Voorhis, M. A. Baldo, *Adv. Mater.* **2017**, *29*, DOI 10.1002/adma.201701987.

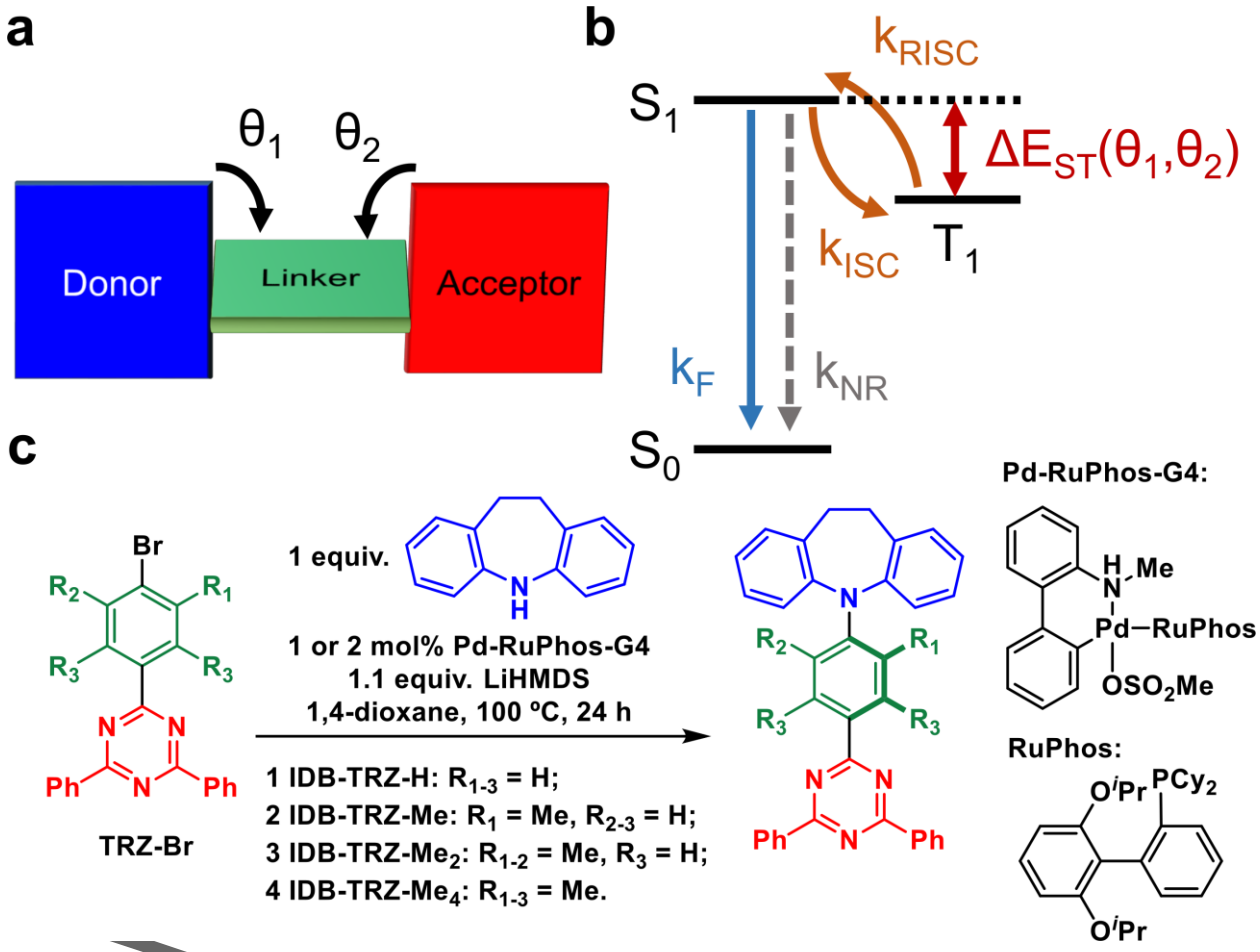

Figure 1. Molecular design strategy. a) Donor-Linker-Acceptor structure with two dihedral angles θ_1 (donor-linker) and θ_2 (linker-acceptor). **b)** Rate model for thermally activated delayed fluorescence (TADF). Singlet-triplet splitting can be tuned by adjusting the dihedral angles. **c)** Synthesis of IDB-TRZ compounds. All IDB-TRZ compounds were synthesized using palladium catalyzed C-N coupling reactions in high yield (87-97%). The donor iminodibenzyl, the acceptor diphenyltriazine, and the linker phenylene are highlighted in blue, red, and green.

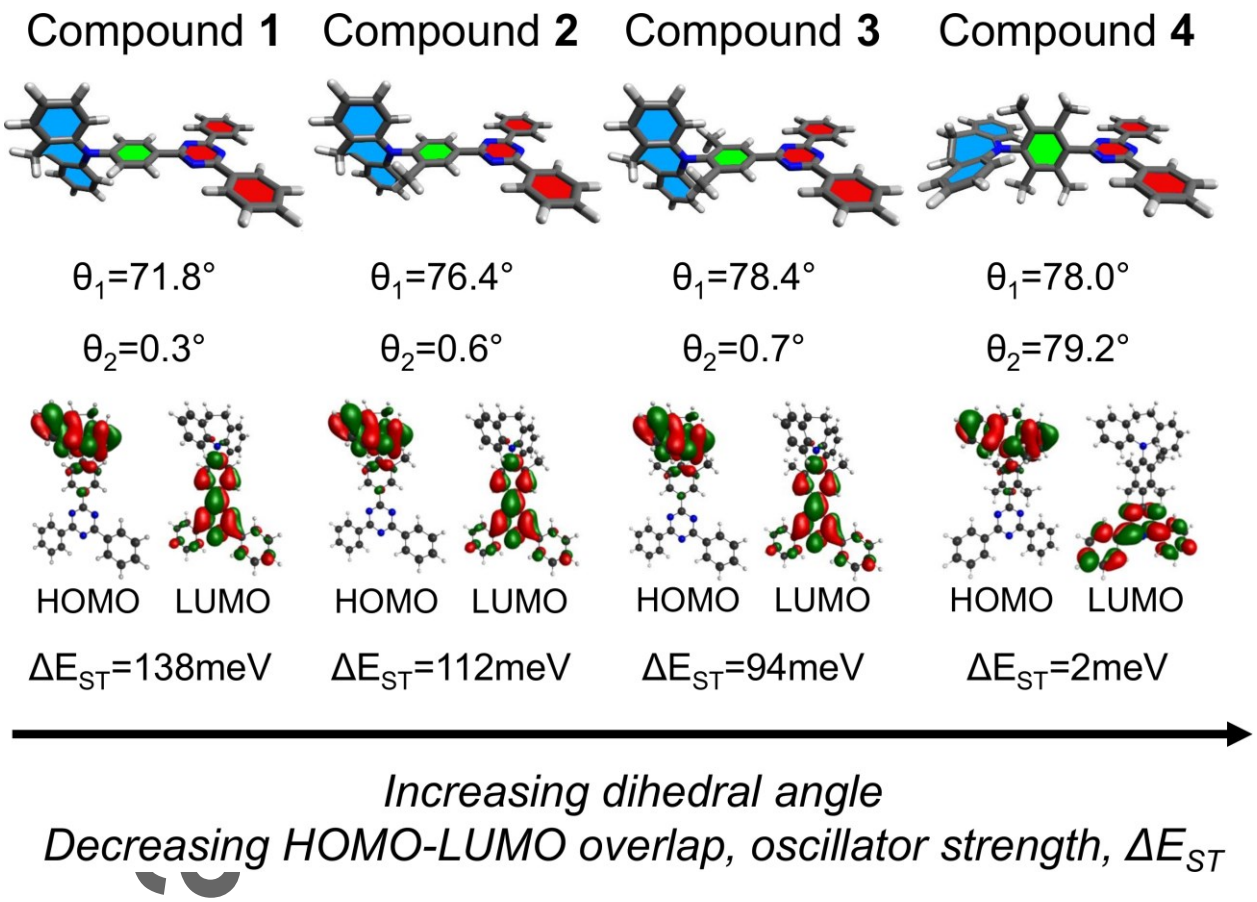

Figure 2: Density functional theory (DFT) results. Optimized geometry, with donor in blue, linker in green and acceptor in red, dihedral angles of iminodibenzyl donor and phenylene linker (θ_1) and phenylene linker and triazine acceptor (θ_2), highest occupied molecular orbital (HOMO) and lowest unoccupied molecular orbital (LUMO), and calculated singlet-triplet splitting ΔE_{ST}.

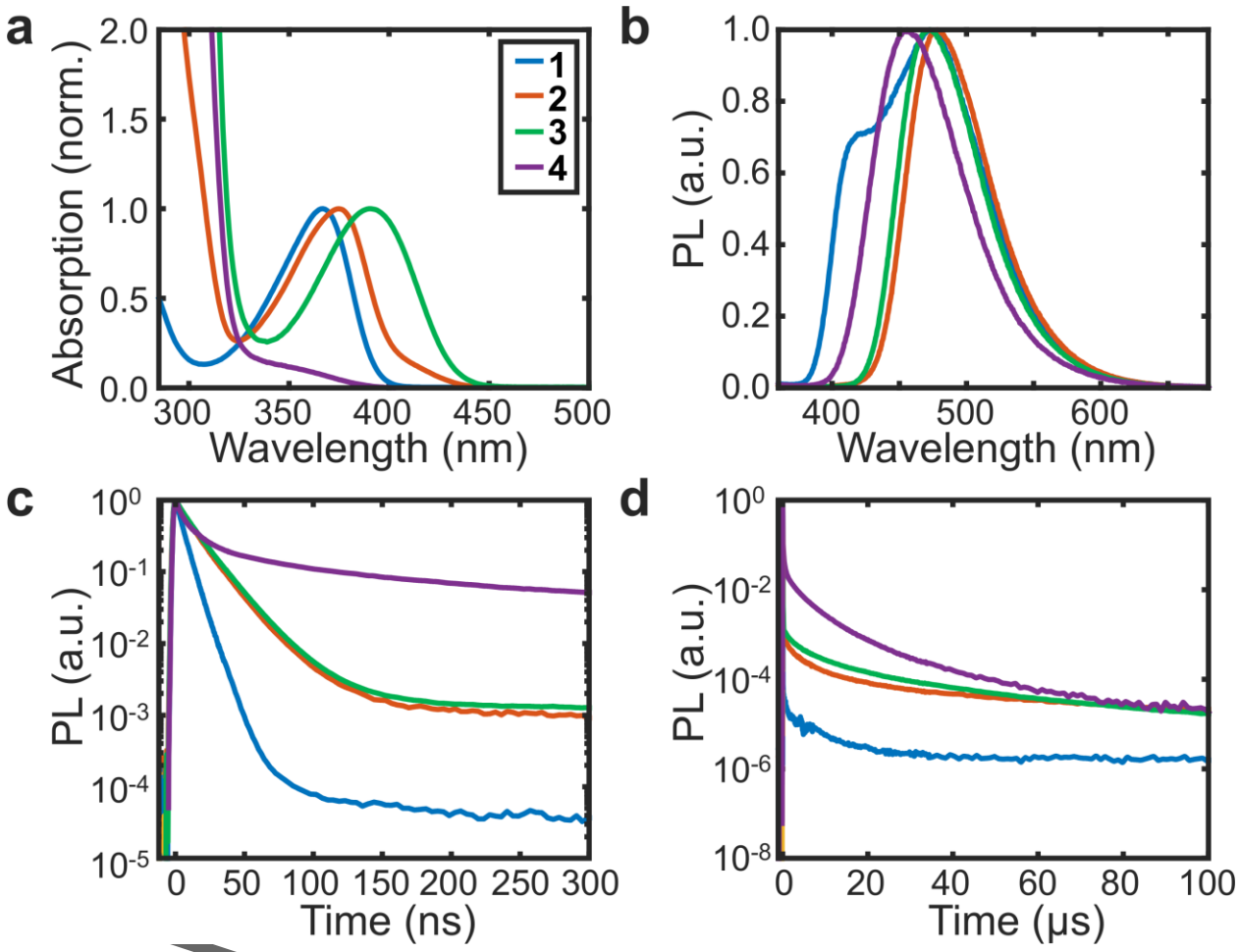

Figure 3: Photophysical properties of compounds 1-4. (a) Normalized absorption spectra. **(b)** Photoluminescence (PL) spectra. **(c)** Time-resolved transient PL: Prompt component. **(d)** Time-resolved transient PL: Delayed component.

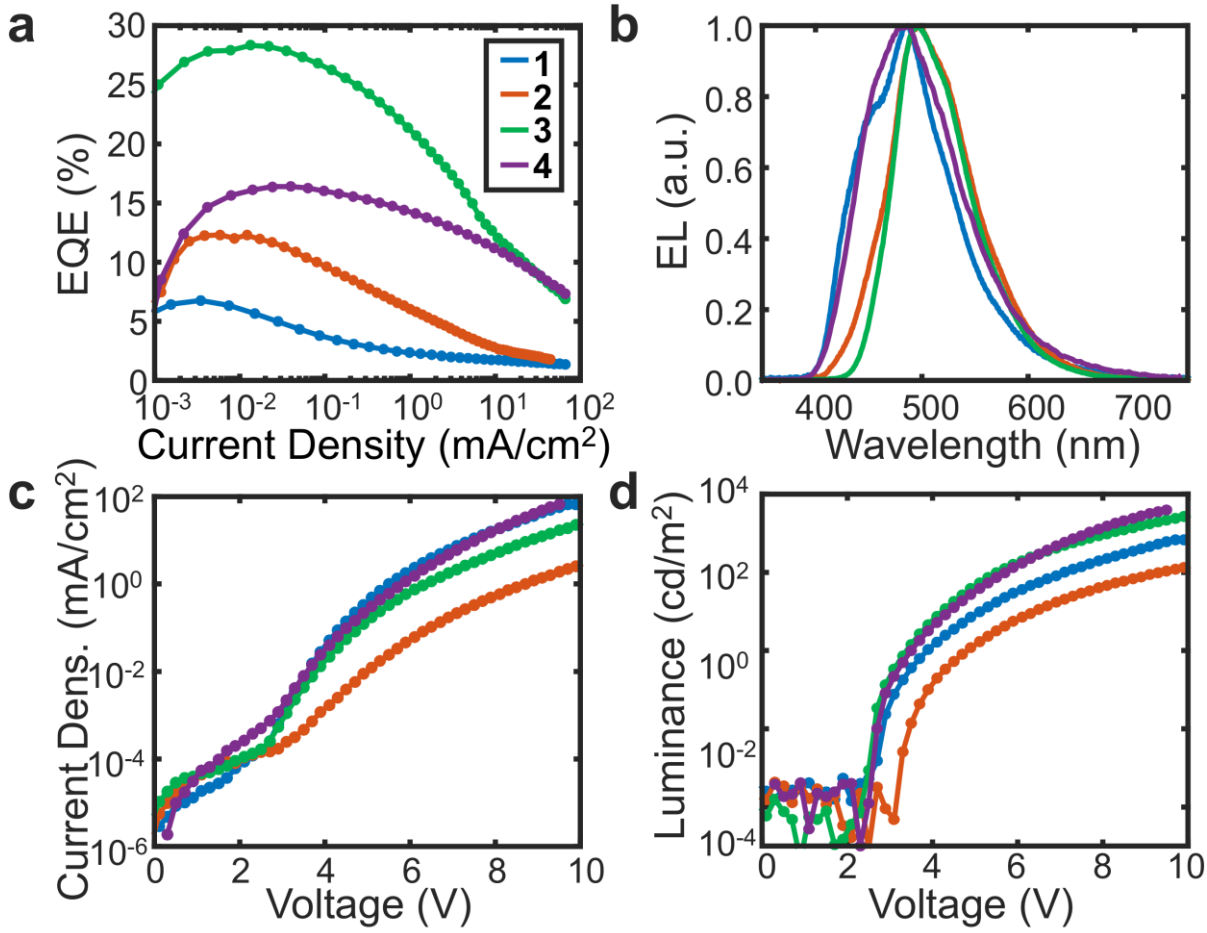

Figure 4: Device performance of compounds 1-4. (a) External Quantum Efficiency (EQE) vs. Current Density. **(b)** Electroluminescence (EL) Spectra. **(c)** Current Density vs. Voltage. **(d)** Luminance vs. Voltage.

Compound	θ_1 [°]	θ_2 [°]	$E(S_1)$ (eV)	$E(T_1)$ (eV)	ΔE_{ST} (meV)	*f*
1	71.8	0.3	2.58	2.44	138[a]/182[b]	0.155
2	76.4	0.6	2.61	2.50	112[a]/93[b]	0.118
3	78.4	0.7	2.65	2.56	94[a]/77[b]	0.093
4	78.0	79.2	2.69	2.69	2[a]/0[b]	0.000

Table 1: Properties of compounds 1-4 as predicted from density functional theory (DFT). θ_1 is the dihedral angle between iminodibenzyl donor and phenylene linker. θ_2 is the dihedral angle between phenylene linker and triazine acceptor. $E(S_1)$ is the energy of the first excited singlet state. $E(T_1)$ is the energy level of the first excited triplet state. ΔE_{ST} is the singlet-triplet gap: a) DFT b) experiment (Figure S8). *f* is the oscillator strength.

Compound	λ_{PL} (nm)	Φ_{PL} (%)	τ_p (ns)	τ_d (µs)	k_{RISC} (10^4 s^{-1})	EQE (%)	λ_{EL} (nm)	CIE (x,y)
1	472	17	7	66	1.7	6.8[a]/1.8[b]	487	0.18,0.25
2	478	68	17	39	4.3	12.3[a]/5.3[b]	496	0.22,0.39
3	472	98	18	28	6.4	28.3[a]/24.2[b]	496	0.21,0.44
4	456	37	22	6	120	16.4[a]/14.4[b]	484	0.20,0.30

Table 2: Photophysical and device properties of compounds 1-4. λ_{PL} is the wavelength of maximum photoluminescence intensity. Φ_{PL} is the photoluminescence quantum yield (PLQY). τ_p is the prompt lifetime. τ_d is the delayed lifetime. k_{RISC} is the reverse intersystem crossing rate. EQE is the external quantum efficiency (EQE) from device measurements: a) maximum EQE; b) EQE at 100 cd/m^2 luminance. λ_{EL} is the wavelength of maximum electroluminescence intensity, CIE denotes the CIE (Commission internationale de l'éclairage) coordinates in the CIE 1931 color space chromaticity diagram.

A series of blue thermally activated delayed fluorescence (TADF) based emitters for organic light-emitting diodes (OLEDs) is presented. By pairing the novel iminodibenzyl donor with the triazine acceptor via a phenylene linker and subsequent tuning of the dihedral angle to the optimal value, a very high external quantum efficiency of 28.3% is achieved. The intricate trade-off between singlet-triplet splitting and fluorescent oscillator strength is explored. The result is a widely applicable molecular design strategy, that can enhance the performance of existing TADF emitters without impairing their emission spectra.